JBC Papers in Press. Published on October 2, 2017 as Manuscript M117.806331
The latest version is at http://www.jbc.org/cgi/doi/10.1074/jbc.M117.806331

A unique cysteine-rich Zn-finger domain present in a majority of class II ribonucleotide reductases mediates catalytic turnover [1]

Christoph Loderer[‡], Venkateswara Rao Jonna[§], Mikael Crona[‡#], Inna Rozman Grinberg[‡], Margareta Sahlin[‡], Anders Hofer[§], Daniel Lundin*[‡], Britt-Marie Sjöberg*[‡]

From the Department of Biochemistry and Biophysics, Stockholm University[‡] and Department of Medical Biochemistry, Umeå University, Sweden[§]; Current address: Swedish Orphan Biovitrum AB, Solna, Sweden[#]

Running title: *Catalytic turnover in class II ribonucleotide reductase*

To whom correspondence should be addressed: Daniel Lundin, telephone: +46-8-52481520, fax: +46-8-155597, daniel.lundin@dbb.su.se; Britt-Marie Sjöberg, telephone: +46-8-164150, fax: +46-8-155597, britt-marie.sjoberg@dbb.su.se

Keywords: ribonucleotide reductase, oligomerization, metal ion-protein interaction, oxidation-reduction (redox), phylogenetics, thioredoxin

ABSTRACT

Ribonucleotide reductases (RNRs) catalyze the reduction of ribonucleotides to the corresponding deoxyribonucleotides, used in DNA synthesis and repair. Two different mechanisms help deliver the required electrons to the RNR active site. Formate can be used as reductant directly in the active site, or gluta- or thioredoxins reduce a C-terminal cysteine pair, which then delivers the electrons to the active site. Here, we characterized a novel cysteine-rich C-terminal domain (CRD), which is present in most class II RNRs found in microbes. The NrdJd-type RNR from the bacterium *Stackebrandtia nassauensis* was used as a model enzyme. We show that the CRD is involved in both, higher oligomeric state formation and electron transfer to the active site. The CRD-dependent formation of high oligomers, such as tetramers and hexamers, was induced by addition of dATP or dGTP, but not of dTTP or dCTP. The electron transfer was mediated by an array of six cysteine residues at the very C-terminal end, which also coordinated a zinc atom. The electron transfer can also occur between subunits, depending on the enzyme's oligomeric state. An investigation of the native reductant of the system revealed no interaction with gluta- or thioredoxins, indicating that this class II RNR uses a different electron source. Our results are indicating that the CRD has a crucial role in catalytic turnover and a potentially new terminal reduction mechanism and suggest that the CRD is important for the activities of many class II RNRs.

Ribonucleotide reductases (RNRs)[2] catalyze the reduction of ribonucleotides to the corresponding deoxyribonucleotides, which are required for DNA synthesis and repair. Since this reaction is the only known biological pathway for *de novo* deoxyribonucleotide synthesis, RNRs are considered to be essential for every living organism. Today, three different classes of RNRs are known, which all share a common fold and a general reaction mechanism based

[1]The work was supported by the Swedish Research Council (2016-01920), Swedish Cancer Society (CAN 2016/670), Wenner-Gren Foundations, Carl Trygger's Foundation and Kempe Foundations.

[2]The abbrevations used are: AdoCbl, adenosylcobalamin; AdoMet, S-adenosyl-L-methionine; CRD, cysteine-rich C-terminal domain; GEMMA, gas phase electrophoretic macromolecule analysis; HED, 2-hydroxyethyl disulfide; ICP, inductively coupled plasma analysis; ICP-OES, inductively coupled plasma optical emission spectrometry; IMAC, metal ion affinity chromatography; ITC, isothermal titration calorimerty; NrdJd-wt, the full-length version of the *Stackebrandtia nassauensis* class II RNR; NrdJdΔCRD, the C-terminally deleted version of the *S. nassauensis* class II RNR; RNR, ribonucleotide reductase; SEC, size exclusion chromatography; TCEP, tris(2-carboxyethyl)phosphine hydrochloride.

on a thiyl radical (1). All known RNRs, except a few viral RNRs, also share an allosteric substrate-specificity regulation, where binding of a dNTP or ATP molecule modulates the specificity of the active site of the enzyme (1). The three classes share a common ancestor (2) and the main difference between them is their mechanism of radical generation (1, 3). With the different radical generating mechanisms follow differences in dependence of oxygen and oligomeric composition.

Class I RNRs (NrdAB/NrdEF) generate the radical in a separate subunit (β, NrdB/F) via a dimetal center that is oxidized by molecular oxygen. The radical is then transferred to the catalytic subunit (α, NrdA/E) and back after the catalytic cycle. Thus, this class is oxygen-dependent and forms active $\alpha_2\beta_2$ heterotetramers. Terminal reduction of the oxidized active site in α is performed by thioredoxin or glutaredoxin systems at the end of each turnover (4, 5).

Class III RNRs (NrdD) also require a separate subunit (NrdG) to generate the radical. An iron-sulfur-cluster in NrdG confers homolytic cleavage of the cofactor *S*-adenosyl-L-methionine (AdoMet) that generates a stable glycyl radical in the catalytic subunit. This glycyl radical is extremely sensitive towards oxygen, leading to protein backbone cleavage at oxygen exposition. NrdDs are described to be active as α_2 homodimers and NrdG is only needed to generate the glycyl radical in NrdD (6, 7). Formate was shown to be a terminal reducing agent for some NrdD enzymes (8). Recently, class III RNRs that use a thioredoxin system for terminal reduction have been described (9).

The RNR that is the focus of the current study, class II (NrdJ), generates the radical via homolytic cleavage of the vitamin B12 coenzyme (AdoCbl) within the enzyme, close to the active site. After the catalytic cycle, AdoCbl is reconstituted (10). This mechanism makes NrdJ enzymes independent of oxygen, but instead dependent on B12. The oligomeric organisation of the NrdJ enzymes is more diverse than in the other classes. Some representatives, such as the enzyme from *Thermoplasma acidophilum*, have been shown to be active as α_2 homodimers (11) whereas the NrdJ from *Lactobacillus leichmannii* is active as monomer, where an additional domain mimics the dimer interface, required for allosteric regulation (12). Higher oligomers have been observed for the full length NrdJ from *Thermotoga maritima*, while a truncated variant utilized for X-ray crystallography crystallized as a dimer (13). The terminal reductant is poorly studied for NrdJ enzymes. The monomeric NrdJ from *L. leichmannii* was shown to receive electrons from thioredoxin (14), but for other NrdJ enzymes reduction by thioredoxin or glutaredoxin has not been studied.

In the monomeric NrdJ, as well as in class I RNRs, the interaction with thioredoxin or glutaredoxin is mediated via a conserved C-terminal cysteine pair. Due to its position on a flexible C-terminal tail, this reduced cysteine pair is believed to have access to the active site and to re-reduce the disulfide that is oxidized during the nucleotide reduction reaction in turn forming a disulfide that is subsequently reduced by the terminal reductant (4, 5). This study reports that most non-monomeric class II RNRs contain a so far undescribed cysteine-rich C-terminal domain (CRD). We show that the CRD is involved in oligomerization and the terminal reduction of the class II RNR from *Stackebrandtia nassauensis* and that the CRD hence plays a crucial role in the catalytic cycle of class II RNRs.

RESULTS

Phylogenetic analysis — We estimated a maximum likelihood phylogenetic tree from an alignment of sequences representing the full diversity of NrdJ sequences at the 75% identity level (Figure 1A; Supporting information). The resolution increased after exclusion of sequences from the monomeric class II enzymes, subclass NrdJm, allowing us to define two well supported, likely monophyletic subclasses (NrdJd, NrdJa+b) with at least one enzymatically characterized member (Figure 1B; Supporting information; http://rnrdb.pfitmap.org). In addition, four likely monophyletic, well supported, candidate subclasses and a number of unclassified sequences were identified. Subclass NrdJm contains the monomeric enzyme from *L. leichmannii* (12), subclass NrdJd contains the enzyme from *Streptomyces clavuligerus* (15) and subclass NrdJa+b contains the split enzyme from *Pseudomonas aeruginosa* (16, 17). Other well characterized NrdJ enzymes such as the one from *T. maritima* and *T. acidophilum* are among the unclassified sequences (11).

An alignment of all NrdJ sequences shows major differences in the C-terminal region. A cysteine-rich C-terminal domain (CRD) is present in 70 % of the investigated sequences. The CRD is 150-220 amino acids long and contains hydrophobic regions with single conserved hydrophilic residues (Figure 1C). The most striking feature of this domain is an array of six fully conserved cysteine residues at the C-terminal end of the sequence (Figure 1C). No sequence similarity between the class I C-terminal sequence, which contains a single pair of conserved cysteines, and the NrdJ CRD was detected.

The CRD is predominant in subclass NrdJd and in three out of the four candidate subclasses as well as in a majority of the unclassified sequences, but not at all in NrdJm. The NrdJa+b subclass consists of enzymes where the CRD is not genetically fused to the catalytic domain, but encoded by a separate gene, *nrdJb*. In some *Frankia* species and a few Alphaproteobacteria, two NrdJd enzymes are present where only one contains the CRD (Suppl. Table S1; http://rnrdb.pfitmap.org).

Recombinant expression of candidate enzymes from subclass NrdJd — To study the properties and the function of the NrdJ subclass in general and the CRD in particular, a set of candidate proteins were identified using a bioinformatic prescreen to estimate successful expression of soluble protein. The NrdJd enzymes from *Streptomyces clavuligerus*, *Coraliomargarita akajimensis* and *S. nassauensis* were selected and recombinantly expressed in *Escherichia coli*. Only the *S. nassauensis* NrdJd showed a sufficient amount of soluble expression of active enzyme with an intact CRD (Figure 2).

In addition, both the isolated catalytic domain of the *S. nassauensis* enzyme (positions 1-714; NrdJdΔCRD), as well as the CRD alone (positions 715-947) were cloned and expressed in *E. coli* separately (Figure 2). The expression of the CRD yielded negligible amounts of soluble protein and aggregation occurred quickly. From the full length enzyme NrdJd-wt and the isolated catalytic domain NrdJΔCRD, soluble protein was obtained in high purity and sufficient quantity. Initial activity assays showed that the enzyme was able to reduce CDP but not CMP or CTP.

Allosteric regulation — An important characteristic of all RNRs known so far, with the exception of class I RNRs from herpes viruses (18), is the allosteric regulation of substrate specificity. Thereby, effector binding in the specificity site in the dimer interface influences the substrate specificity of the active site. The potential effectors ATP, dATP, dCTP, dGTP and dTTP were tested for their influence on the reduction of ADP, CDP, GDP and UDP by NrdJd-wt and NrdJdΔCRD. All four potential substrates were present in the assay together with one of the five potential effector molecules at a time and conversion of all substrates was measured. The effectors ATP and dATP activated the wild type enzyme for CDP reduction (Figure 3A). dCTP and dTTP enhance the activity for GDP reduction, while dGTP activates both enzymes for ADP and GDP reduction. UDP conversion was not observed with any of the tested effector nucleotides. Except for a low activity with ATP as effector, the experiment yielded similar results for NrdJdΔCRD (Figure 3B). To investigate the affinity of NrdJd-wt and NrdJdΔCRD towards the preferred effectors, activity assays with a single substrate were performed in presence of increasing effector concentrations. For NrdJd-wt all effectors yielded nearly maximal activity already at the lowest tested effector concentration of 4 μmol L^{-1} (Figure 3C). This concentrations represents only a two fold molar excess over the applied enzyme concentration of 2 μmol L^{-1}. This indicates very low K_L-values (< 4 μmol L^{-1}), but it also means that the actual values cannot be determined based on activity at these conditions. For NrdJdΔCRD the effector titrations yielded saturation curves with K_L-values between 50 and 150 μmol L^{-1} (Figure 3D). In conclusion, the affinity of the C-terminally truncated enzyme towards each tested effector is reduced. However, the overall pattern of activation or inactivation of the enzyme for different substrates by the effectors is intact.

Oligomeric state — The oligomeric state of *S. nassauensis* NrdJd was studied using size exclusion chromatography (SEC) at high protein concentration (1.0 mg mL^{-1}) and gas phase electrophoretic macromolecule analysis (GEMMA) at a lower con-

centration (0.075 mg mL^{-1}). The latter is comparable to the enzyme concentration in the activity assays. The full length NrdJd yielded a SEC peak at 450 kDa, corresponding to a tetramer that was unaffected by dATP addition (Figure 4A). In GEMMA, NrdJd-wt shows a mixture of monomers and dimers, that shifts to a tetramer only in the presence of 100 µmol L^{-1} dATP (Figure 4C). NrdJdΔCRD, on the other hand, is present as a monomer between 90-100 kDa both in SEC and in GEMMA (Figure 4B,D). The NrdJdΔCRD monomer and the small fraction of dimer visible in GEMMA were not affected by the addition of dATP (Figure 4D). dGTP yielded results similar to dATP, whereas addition of dTTP (Figure 4C) and dCTP induced dimerization but not tetramerization in NrdJd-wt. In titrations with dATP, as well as dGTP, NrdJd-wt was in a monomer-dimer equilibrium at lower concentrations of the effector and gradually changed to tetramers and even hexamers when the effector concentration was increased (Figure 4E,F). By interpolation of the quantified GEMMA results based on mass concentration, half the enzyme is present as tetramer or hexamer at a concentration of 17 µmol L^{-1} dATP.

Electron transfer — Since two C-terminal cysteine residues are known to be the acceptors of electrons from glutaredoxins and thioredoxins in the class I and NrdJm enzymes, the role in electron transfer of the *S. nassauensis* NrdJd CRD and its six cysteine residues was investigated. Earlier studies with alternative reducing systems have demonstrated that the phosphine TCEP specifically reduces the C-terminal cysteine residues of class I RNR, while DTT can reduce the enzyme active site directly (19). In this study *S. nassauensis* NrdJd-wt and NrdJdΔCRD were tested with both reductants (Figure 5). NrdJd-wt activity is supported by both DTT and TCEP, with four-fold higher specific activity using the latter. NrdJdΔCRD exhibits a comparable activity with the reductant DTT as the wild-type enzyme, but is completely inactive with TCEP. An attempted reconstitution of the full length protein with equimolar amounts of NrdJdΔCRD and the separately expressed CRD did not show any activity with TCEP (data not shown).A PROSITE search did not fit the *S. nassauensis* CRD to any known cysteine-rich motif such as zinc fingers. On the other hand, a sequence similarity search against the PDB database (http://www.rcsb.org/pdb/home/home.do) suggested similarity to a zinc binding site from tRNA(Ile2) 2-agmatinylcytidine synthetase (PDB: 4RVZ) from *Archaeoglobus fulgidus* (20). Based on this structure, a homology model of the *S. nassauensis* C-terminal 35 residues was created applying Swiss Model (Figure 6A).

The model suggested that a zinc is coordinated by the cysteine residues C920, C923, C936 and C939 (Figure 6B). The remaining two cysteine residues C933 and C945 are in close proximity in the model and could form the site of terminal reduction. This homology model was applied as a starting model for subsequent experimental confirmation. Accordingly, six different cysteine to alanine substitution variants of *S. nassauensis* NrdJd were constructed and their enzyme activity tested in assays applying either DTT or TCEP as reductants. All variants retained at least 50% of their specific activity with the reductant DTT (Figure 6C). However, none of the variants besides the wild type showed any enzyme activity with the reductant TCEP, suggesting all cysteines are essential for active site reduction.

In an attempt to assess the four cysteine residues that are suggested to coordinate zinc, inductively coupled plasma (ICP) measurements were performed for the wild type enzyme and all six cysteine to alanine mutants (Figure 6C). The wild-type enzyme as well as the variants C933A and C939A showed a zinc occupation of more than 60% per monomer. The variants C920A, C923A and C936A yielded reduced occupancy to between 20% and 40%, while C945A was fully occupied. Thus, the exchange of the two cysteine residues predicted to form the terminal cysteine pair had comparable or higher Zn^{2+} occupation than the wild type whereas of the four cysteine residues predicted to coordinate the zinc, three showed a reduced zinc content, while one was equal to the wild type.

Subunit crosstalk — The CRD is responsible for electron delivery to the active site but as shown above, the NrdJd can adopt different oligomeric states. This leads to the question whether the C-terminal cysteine residues can only reach the active site of their own subunit or if they can also deliver electrons to other subunits within the oligomer. To investigate this, an active site cysteine deficient mu-

tant (C370A) was mixed in equimolar amounts with a C-terminal mutant protein. In control experiments the C370A mutant showed no activity with any of the reductants, TCEP or DTT, while the C-terminal mutant C933A was active with DTT but not with TCEP (Figure 7A). Yet the mixture of the two mutant proteins exhibited high enzyme activity with both DTT or TCEP, indicating electron transfer from the intact C-terminus of the active site mutant C370A to the active site of the CRD mutant C933A.

Due to the complex oligomeric organization of NrdJd-wt, the influence of the oligomeric state on the subunit crosstalk was investigated. Activity assays were performed with the wild type enzyme and the mixture of the CRD mutant C933A and active site mutant C370A. To test for crosstalk in the dimer, the substrate/effector pair GDP/dTTP was applied, where no formation of higher oligomers was observed in the previous experiments. Crosstalk in higher oligomers was investigated, using the substrate/effector pair CDP/dATP, where formation of tetramers and hexamers was shown in the GEMMA experiments (Figure 7B). In both cases TCEP was applied as reductant. NrdJd-wt had a low K_L-value < 4.0 μmol L^{-1} for dATP. For the C933A/C370A mixture, an increased K_L-value of 15.0 ± 4.5 μmol L^{-1} was determined. The V_{max} value in the variant mixture was reduced to 30% of the wild type, which is close to the theoretical maximum value of 50% considering that half of the subunits in the mixture has a defective active site. For the effector dTTP, NrdJd-wt showed maximum activity already at the lowest dTTP concentration, indicating a high affinity. The C933A/C370A mixture exhibited very low overall activity between 3 and 7% of NrdJd-wt with no significant effect of increasing dTTP concentrations. To further assess the effect of dATP, assays were performed with mixtures of dATP and dTTP (Figure 7C). For both the C933A/C370A mixture and NrdJd-wt, activity with the substrate CDP was lower in the presence of dATP plus dTTP compared to dATP alone. However, the addition of 250 μmol L^{-1} dATP to 1 mmol L^{-1} dTTP lead to an increase in GDP reduction for the C933A/C370A mixture and NrdJd-wt. The effect was especially pronounced in the C933A/C370A mixture, where activity increased 18-fold compared to 4-fold in the wild-type enzyme.

Native electron donor — To further investigate the role of the C-terminal cysteine residues as terminal reducing sites of the enzyme, we attempted to define the native reductant. In many class I RNRs as well as for the NrdJm from *L. leichmannii*, thioredoxins and glutaredoxins serve as native reductants (1, 14). Therefore, we performed a sequence similarity search for thio- and glutaredoxins in the *S. nassauensis* proteome. The organism encodes two thioredoxins, Snas 2647 (thioredoxin 1) and Snas 6430 (thioredoxin 2), as well as one glutaredoxin, Snas 1785. The three redoxins, together with the thioredoxin reductase (TR) Snas 6431, were cloned and recombinantly expressed in *E. coli*. All constructs yielded soluble protein in high amounts with high specific activities on artificial substrates (Figure 8A). All thio- and glutaredoxins were tested in the RNR activity assay together with their corresponding electron source (thioredoxin reductase + NADPH for the thioredoxins, and glutathione + glutathione reductase + NADPH for glutaredoxin). However, no RNR activity was detected in presence of any of the redoxin systems (Figure 8B). To test whether the conditions for the combined assay are suitable for RNR and the redoxin systems, both reaction systems were monitored separately. Addition of the artificial reductant DTT to the full reaction mix resulted in high specific activity of the RNR (Figure 8B). Addition of the artificial electron acceptors insulin (thioredoxins) and HED (glutaredoxin) yielded high specific activities for the redoxin systems (Figure 8A). Both the RNR and the redoxin systems, exhibited high activity at the combined assay conditions, but no transfer of electrons could be observed between them.

In another attempt to identify the native electron donor, RNR assays were performed with different types of *S. nassauensis* cell lysates (Figure 8C). Tests were performed with protein-free lysate (1), cleared lysate (2) and complete lysate (3). None of the lysates increased activity beyond the level measured in the negative control.

DISCUSSION

We characterized a unique C-terminal cysteine-rich domain, present in a majority of class

II RNRs, which is involved in oligomerization and terminal reduction during catalysis. This domain is identical to the NrdJb subunit in the NrdJa+b split enzyme described for *P. aeruginosa* (16, 17) and the CRD that was spontaneously cleaved from *T. maritima* NrdJ, used for crystallization (13). Sequence analysis revealed the presence of the CRD in 70% of the non redundant NrdJ sequences, excluding the monomeric NrdJm which never contains the CRD (Figure 1B; Supplementary Table S1). Among the non-monomeric NrdJs, the presence of the CRD does not follow a simple phylogenetic pattern (Figure 1A,B). The domain is present in the majority of subclasses and candidate subclasses. Absences are spread throughout the tree, suggesting independent losses of the domain. In NrdJd, the only absences of the CRD we could detect, were from genomes also encoding another NrdJd with a CRD.

The high occurrence of the CRD-domain in NrdJ enzymes, as well as its genetic separation from the catalytic subunit in NrdJa+b, indicate not only the general importance of the domain but also that it is a separately folded independent domain. Previous studies of enzymes containing the CRD have suffered from the aggregation-promoting properties of this domain as well as its susceptibility to cleavage (11, 17). For the genetically separate CRD, NrdJb from *P. aeruginosa*, it was not possible to obtain soluble protein by heterologous expression in *E. coli* (17). Recombinant expression of the full length unclassified NrdJ from *T. maritima* yielded soluble protein but the CRD was partially cleaved during expression (13). Fortunately, the NrdJd from *S. nassauensis* did not show any sign of cleavage during expression or further experiments.

Our functional analysis of the CRD suggests an important role in oligomerization and electron transfer. The CRD-dependend formation of higher oligomers is well in line with observations made for the NrdJ from *T. maritima*, which was first characterized as a higher oligomer with about 450 kDa (11). The C-terminally truncated version was later characterized as a dimer (13). In this study, we show that the C-terminally truncated NrdJ enzyme from *S. nassauensis* is in a monomer-dimer equilibrium. Tetramers and hexamers were only observed in the full length enzyme, showing the importance of the CRD for the formation of higher oligomers. Experiments also showed that this oligomerization is stimulated by addition of the purine nucleotides dATP and dGTP, but not by the pyrimidine nucleotides dTTP and dCTP.

While the actual mechanism behind the CRD's role in oligomerization and how this affects activity of the enzyme still remains to be described, the role of the CRD in the re-reduction of the active site cysteine residues is much clearer. Although sequence similarity between the CRD of most NrdJs on one side and the C-termini of Class I RNRs and monomeric NrdJs on the other side is limited to a single pair of cysteines, the mechanism appears comparable (4, 5, 14). This is supported by the inability of NrdJdΔCRD to accept TCEP as terminal reductant while activity is retained with DTT, the latter being small enough to directly reduce the active site whereas the former is not (19).

The TCEP experiments with the six cysteine-to-alanine exchanges showed that all six cysteine residues are necessary for the functionality of the electron transfer. Homology modeling indicated that four of these cysteine residues (C920, C923, C936, C939) could be involved in zinc binding while the remaining two (C933, C945) appear to form the redox-active cysteine pair. However, the ICP measurement only shows reduced zinc content in three of the four predicted positions. A zinc occupancy between 0.2 and 0.4 in the variants, compared to 0.6 in the wild type enzyme, is in good agreement with values measured in comparable studies (21, 22). It is noteworthy, that both C933A and C939A show the same zinc content as the wild type, while it is reduced in C936A. Possibly, the zinc can be coordinated either by C933-C936 or C936-C939. Both these pairs have the common sequence C-X-X-C that is typical of zinc ligating cysteines. A certain promiscuity in the coordination of the zinc would also explain why no single mutant showed a complete loss of zinc as observed in the full truncation. Taking the potential swap between C933 and C939 into account, the results are consistent with the homology model. We thus propose, that the residues C920, C923, C936 and C939 coordinate a zinc residue, structuring the C-terminal end and bringing C933 and C945 in close proximity to each other. This pair can then act as an electron shuttle between the electron donor and the active site. Coordination

of the zinc by C933 in case of the C939A variant seems possible, in which case a restructured metal binding site could still bind the zinc ligand, but C945 would be deprived of its partner, prohibiting the role of terminal reduction.

A C-terminal zinc binding site was previously described for NrdD enzymes (23, 24). It was proposed to be a structure forming element, which keeps the catalytically crucial glycyl radical in correct orientation. Due to the low sequence similarity and the very different location of the zinc binding site within the sequences, there is no evidence for homology between the sites in class II and class III RNRs. Cysteine-coordinated zincs with a structural role are commonly found in proteins (25, 26) and are often the result of convergent evolution.

With the help of mutant proteins defective in the active site (C370A) and in the CRD (C933A), we demonstrated electron transfer from the CRD of one subunit to the active site of another subunit. The effects of oligomerization on this crosstalk were investigated by addition of the effectors dATP and dTTP with their different oligomerization effects. The results indicate that an efficient transfer of electrons between the subunits can occur only in tetramers or higher oligomers. The measured K_L-value for dATP of 15 μmol L^{-1} compares well with the GEMMA results where, at an estimated concentration of 17 μmol L^{-1}, half of the enzyme is present as tetramer or higher oligomer. Crosstalk between terminal reduction sites has been observed before in the class I RNR from *S. cerevisiae* and suggestded to occur within the dimer. (27). Higher oligomerization that allows for tuning of electron transfer between the subunits could represent a novel layer of activity regulation.

In GEMMA experiments and activity assays all four dNTPs were shown to induce dimerization and act as effectors via the specificity site but the formation of higher oligomers was induced only by dATP and dGTP. We therefore sought to study whether there is an additional effector binding site, different from the specificity site. Attempted direct binding assays and ITC experiments did not yield conclusive results (data not shown), but experiments with mixtures of effectors were indicative of a third nucleotide binding site. While addition of dTTP to a CDP/dATP assay inhibited enyzme activity in accordance with the described allosteric regulation, addition of dATP to a GDP/dTTP assay instead led to an increase in activity. However, dATP does not activate GDP reduction via the described allosteric mechanism. Instead, it suggests that dATP binding to another site may mediate the increase in activity by formation of higher oligomers.

To assess the physiological role of the CRD, we attempted to find the native electron donor of the system. The three tested gluta- and thioredoxins from *S. nassauensis* were not able to supply the RNR with electrons under the tested conditions. The observation that all systems separately, the RNR and the gluta-/thioredoxin systems, are active but cannot exchange electrons, questions whether RNRs with the CRD are dependent on reduction by a redoxin system at all. Attempts to find the native electron donor in *S. nassauensis* cell lysates did, however, not yield any positive results. Since the organism also contains a class I RNR, the native electron donor system might not be expressed during the employed culture conditions or might be inactivated in the lysis process. As shown by Berardi and Bushweller in NMR studies, the very flexible, disordered C-terminal tail of class I and NrdJm enzymes plays a vital role in the interaction of the C-terminal cysteine residues with the redoxins (28). The highly ordered C-terminus in CRD-containing NrdJ enzymes might be unsuitable for an interaction with redoxins in a fashion comparable to class I or NrdJm RNRs. Our so far unproductive attempts to find the reducing system for *S. nassauensis* together with the recent discovery that some class III RNRs are indeed reduced by redoxins (9), and not by formate that was long believed to be the sole reductant of these enzymes, show the plurality of ultimate reductants that can be involved in ribonucleotide reduction.

EXPERIMENTAL PROCEDURES

Bioinformatics — All full-length NrdJ sequences in RefSeq were downloaded from RNRdb (http://rnrdb.pfitmap.org) (2017-02-17) and clustered at 75% identity with USEARCH (29) to create a selection of representative sequences. Sequences were aligned with Probcons (30) and reliable alignment positions were selected with BMGE (31) using

the BLOSUM30 model. A phylogeny was estimated with RAxML (32) in rapid bootstrapping mode with automatic bootstopping (extended majority rule) using the PROTGAMMAAUTO model. An HMM profile for the CRD domain was constructed from the CRD domain found in 217 sequences in the alignment used for phylogenetic estimation. The Skylign server was used to graphically represent the profile as a sequence logo (33).
Secondary structure prediction was performed with the Chou & Fasman Secondary Structure Prediction Server (CFSSP) (34, 35). The homology model of the C-terminus was constructed via the Swiss model server (36–39). After automated template search, a model was built based on the template with the highest sequence identity. For the model discussed above, the 35 amino acid C-terminus of tRNA(Ile2) 2-agmatinylcytidine synthetase from *A. fulgidus* (PDB: 4RVZ) with a sequence identity of 31% was applied as template.

Molecular cloning — The genes from the NrdJd from *S. nassauensis* (Snas 4560; full length and CRD) and *S. clavuligerus* (AJ224870) as well as the genes from the thioredoxins (Snas 6430, Snas 2647), the glutaredoxin (Snas 1785) and the thioredoxin reductase (Snas 6431) were amplified from genomic DNA via PCR. All genes were cloned into a pET22b(+) vector via NdeI and HindIII restriction sites adding a N-terminal His-tag connected via a thrombin restriction site. For recombinant expression, the vectors were transformed in *E. coli* BL21(DE3).

Mutagenesis — The C-terminal truncation of the NrdJd from *S. nassauensis*, NrdJdΔCRD, as well as all cysteine to alanine mutations were performed via site-directed mutagenesis using mismatched oligonucleotides. For NrdJdΔCRD the GAG bases coding for Glu715 were exchanged by a TAA stop codon. For the cysteine to alanine mutations the TGC and TGA codons for cysteine were replaced by GCA coding for alanine.

Recombinant expression and purification — Expression was performed in LB-medium in 600 mL scale in baffled shake flasks. The medium was inoculated from a preculture to a starting OD_{600} of 0.05-0.1 and incubated at 37°C and 150 RPM. After reaching an OD_{600} of 0.8 the temperature was decreased to 15°C (NrdJds and truncations) or 20°C (glutaredoxin, thioredoxins and thioredoxin reductase) After induction with IPTG with a final concentration of 0.1 mmol L^{-1}, the cultures were incubated for 4 h (NrdJds and truncations) or 18 h (glutaredoxin, thioredoxins and thioredoxin reductase). Cells were then harvested by centrifugation.
Cell lysis was performed in HisWash buffer (50 mmol L^{-1} Tris pH 7.5, 300 mmol L^{-1} NaCl, 20 mmol L^{-1} imidazole, 1 mmol L^{-1} DTT) by high pressure homogenization three times at 15 MPa. Purification was performed via Immobilized metal ion affinity chromatography (IMAC). The supernatant from the cell lysis was applied on a HisTrap column washed with HisWash buffer and eluted with HisElute buffer (50 mmol L^{-1} Tris pH 7.5, 300 mmol L^{-1} NaCl, 500 mmol L^{-1} imidazole, 1 mmol L^{-1} DTT).
In a second purification step, elution fractions from the IMAC were loaded on Highload™ 16/600 Superdex 200 pg gel filtration column and run with SEC buffer (50 mmol L^{-1} Tris pH 7.5, 300 mmol L^{-1} NaCl, 1 mmol L^{-1} DTT). If not used immediately, purified proteins were frozen in $N_{2(liq)}$ and stored at -80°C.

Analytical size exclusion chromatography (SEC) — SEC for analytical purposes were run on a Superdex™ increase 200 3.2 column. 25 µL of protein sample with a concentration of 1.0 mg mL^{-1} were injected into the column and run with SEC buffer (50 mmol L^{-1} Tris pH 7.5, 300 mmol L^{-1} NaCl, 1 mmol L^{-1} DTT) in the presence or absence of 100 μmol L^{-1} effector.

Gas-phase electrophoretic mobility molecular analyzer (GEMMA) — GEMMA experiments were performed on TSI3480 electrospray aerosol generator, TSI3080 electrostatic classifier and TSI3025A ultrafine condensation particle counter. The buffer of the protein samples was changed to 40 mmol L^{-1} ammonium acetate (pH 7.5) via a desalting column. Substrates and effectors were added to the protein sample with an equimolar amount of $MgCl_2$. The samples were run in the final conditions: 40 mmol L^{-1} ammonium acetate (pH 7.8),

0.005% Tween 20, 0.2 mmol L^{-1} DTT, 100 µmol L^{-1} effector, 100 μmol L^{-1} substrate. The final concentrations of the proteins applied were 0.075 mg mL^{-1} for *S. nassauensis* NrdJd full length and 0,025 mg mL^{-1} for NrdJdΔCRD. The samples were run at a pressure of 1.7 PSI, a current of 160-200 nA and a voltage of 1.8 - 2.0 kV. For data collection, five runs per sample were conducted.

Enzyme activity assay — Specific enzyme activities were determined by measurement of the conversion of NDP to dNDP, catalyzed by the enzyme in the presence of different dNTPs as allosteric effectors. All enzymatic assays were performed in triplicates. Under standard conditions the assay contains 50 mmol L^{-1} Tris (pH 8.0), 20 mmol L^{-1} $MgCl_2$, 50 mmol L^{-1} DTT, 1.0 mmol L^{-1} dATP, 2.0 mmol L^{-1} CDP, 5.0 µmol L^{-1} AdoCbl and between 2 and 5 µmol L^{-1} enzyme (0.2-0.5 mg mL^{-1}). In effector titration experiments, a concentration range from 4 to 1000 µmol L^{-1} was applied, including a measurement without effector. In the four substrate assays, 0.5 mmol L^{-1} of each substrate (ADP, CDP, GDP, UDP) were applied with 0.5 mmol L^{-1} of the tested effector. The assays, performed in 50 μL scale, were incubated 15 or 30 min at room temperature and stopped by addition of 50 μL methanol. After addition of 200 µL water, the samples were analyzed via HPLC. 20 μL of the sample were injected onto a C18 column and run with the following buffer: 50 mmol L^{-1} KP_i (pH 7.5), 10% (v/v) methanol, 0.25% (v/v) tetrabutylammonium hydroxide. The buffer was prepared with KH_2PO_4 by setting the pH value with KOH. The analytes were eluted in a linear gradient of methanol from 10 - 30% (v/v).
Photometric assays for thioredoxins and glutaredoxins based on the artificial electron acceptors Insulin and HED were performed as described in earlier studies (40, 41). The thioredoxin assay contains 50 mmol L^{-1} Tris (pH 8.0), 20 μmol L^{-1} thioredoxin, 1 μmol L^{-1} thioredoxin reductase, 750 μg mL^{-1} insulin and 250 μmol l^{-1} NADPH. The glutaredoxin assay contains 50 mmol L^{-1} Tris (pH 8.0), 20 μmol L^{-1} glutaredoxin, 7.5 U mL^{-1} glutathione reductase, 1 mmol L^{-1} glutathione, 750 μmol l^{-1} HED and 250 μmol l^{-1} NADPH. All assays were run in triplicates for 5 min at room temperature.
In the combined redoxin/RNR assays all reaction components for the single RNR and redoxin assays were combined with the following adjustments: 5 μmol L^{-1} RNR, 5 mmol L^{-1} glutathione, 20 μmol L^{-1} thioredoxin/glutaredoxin. The assays were incubated for 30 min at room temperature and analyzed photometrically as well as by HPLC as described above.

Inductively coupled plasma mass spectrometry (ICP) — ICP measurements were performed at the Z.B.M. - Analytical Laboratory at the Hebrew University of Jerusalem. ICP-OES analysis was performed after an acidic hot block digestion. ICP-OES measurements were performed in triplicates applying yttrium as internal standard.

Acknowledgments: We thank Fredrik Tholander for generously sharing his HPLC-based RNR assay method and equipment with us, and Vasiliy Rosen for the performance of the ICP experiments at Hebrew University of Jerusalem. We also thank the two anonymous revierwers for their constructive revision of our manuscript. The work was supported by the Swedish Research Council (2016-01920), Swedish Cancer Society (CAN 2016/670), Wenner-Gren Foundations, Carl Trygger's Foundation and Kempe Foundations.

Conflict of interest: No conflict of interest declared.

Author contributions: The concept of the manuscript and the writing were performed by CL, DL and BMS. CL performed a large part of the experimental work. DL and BMS performed the phylogenetic investigation of class II RNRs. VRJ and AH helped with the performance and interpretation of the GEMMA experiments. IRG and MS contributed in the production and characterization of the studied enzymes. MC established and performed HPLC analytics and helped interpreting the results. All authors critically reviewed the manuscript and approve with its publication.

REFERENCES

1. Nordlund, P. and Reichard, P. (2006) Ribonucleotide reductases. *Annu. Rev. Biochem.* **75**, 681–706.
2. Lundin, D., Berggren, G., Logan, D. T., and Sjöberg, B. M. (2015) The origin and evolution of ribonucleotide reduction. *Life* **5**(1), 604–636.
3. Stubbe, J., Nocera, D. G., Yee, C. S., and Zhang, M. C. Y. (2003) Radical initiation in the class I ribonucleotide reductase: long-range proton-coupled electron transfer. *Chem. Rev.* **103**, 2167–2201.
4. Åberg, A., Hahne, S., Karlsson, M., Larsson, Å., Ormö, M., Åhgren, A., and Sjöberg, B. M. (1989) Evidence for two different classes of redox-active cysteines in ribonucleotide reductase of Escherichia coli. *J. Biol. Chem.* **264**(21), 12249–12252.
5. Mao, S. S., Yu, G. X., Chalfoun, D., and Stubbe, J. (1992) Characterization of C439SR1, a mutant of Escherichia coli ribonucleotide diphosphate reductase: evidence that C439 is a residue essential for nucleotide reduction and C439SR1 is a protein possessing novel thioredoxin-like activity. *Biochemistry* **31**(40), 9752–9759.
6. Logan, D. T., Andersson, J., Sjöberg, B. M., and Nordlund, P. (1999) A glycyl radical site in the crystal structure of a class III ribonucleotide reductase. *Science* **283**, 1499–1504.
7. Torrents, E., Buist, G., Liu, A., Eliasson, R., Kok, J., Gibert, I., Gräslund, A., and Reichard, P. (2000) The anaerobic (class III) ribonucleotide reductase from Lactococcus lactis. *J. Biol. Chem.* **275**(4), 2463–2471.
8. Mulliez, E., Ollagnier, S., Fontecave, M., Eliasson, R., and Reichard, P. (1995) Formate is the hydrogen donor for the anaerobic ribonucleotide reductase from Escherichia coli. *Proc. Natl. Acad. Sci. USA* **92**, 8759–8762.
9. Wei, Y., Li, B., Prakash, D., Ferry, J. G., Elliott, S. J., and Stubbe, J. (2015) A ferredoxin disulfide reductase delivers electrons to the Methanosarcina barkeri class III ribonucleotide reductase. *Biochemistry* **54**(47), 7019–28.
10. Lawrence, C. C. and Stubbe, J. (1998) The function of adenosylcobalamin in the mechanism of ribonucleoside triphosphate reductase from Lactobacillus leichmannii. *Curr. Opin. Chem. Biol.* **2**, 650–655.
11. Eliasson, R., Pontis, E., Jordan, A., and Reichard, P. (1999) Allosteric control of three B12-dependent (class II) ribonucleotide reductases. *J. Biol. Chem.* **274**(11), 7182–7189.
12. Sintchak, M. D., Arjara, G., Kellogg, B. A., Stubbe, J., and Drennan, C. L. (2002) The crystal structure of class II ribonucleotide reductase reveals how an allosterically regulated monomer mimics a dimer. *Nat. Struct. Biol.* **9**(4), 293–300.
13. Larsson, K. M., Jordan, A., Eliasson, R., Reichard, P., Logan, D. T., and Nordlund, P. (2004) Structural mechanism of allosteric substrate specificity regulation in a ribonucleotide reductase. *Nat. Struct. Mol. Biol.* **11**(11), 1142–1149.
14. Booker, S., Licht, S., Broderick, J., and Stubbe, J. (1994) Coenzyme B12-dependent ribonucleotide reductase: evidence for the participation of five cysteine residues in ribonucleotide reduction. *Biochemisty* **33**, 12676–12685.
15. Borovok, I., Schreiber, R., Holmgren, A., Kreisberg-Zakarin, R., Myslovati, M., Cohen, G., Yanko, M., Åslund, F., and Aharonowitz, Y. (2002) Streptomyces spp. contain class Ia and class II ribonucleotide reductases: expression analysis of the genes in vegetative growth. *Microbiology* **148**, 391–404.
16. Torrents, E., Poplawski, A., and Sjöberg, B. M. (2005) Two proteins mediate class II ribonucleotide reductase activity in Pseudomonas aeruginosa: expression and transcriptional analysis of the aerobic enzymes. *J. Biol. Chem.* **280**(17), 16571–16578.
17. Crona, M., Hofer, A., Astorga-Wells, J., Sjöberg, B. M., and Tholander, F. (2015) Biochemical characterization of the split class II ribonucleotide reductase from Pseudomonas aeruginosa. *PLoS*

One **10**(7), e0134293.

18. Averett, D. R., Lubbers, C., Elion, G. B., and Spector, T. (1983) Ribonucleotide reductase induced by Herpes simplex type 1 virus. *J. Biol. Chem.* **258**(16), 9831–9838.
19. Domkin, V. and Chabes, A. (2014) Phosphines are ribonucleotide reductase reductants that act via C-terminal cysteines similar to thioredoxins and glutaredoxins. *Sci. Rep.* **4**, 5539.
20. Li, F., Dong, J., Hu, X., Gong, W., Li, J., Shen, J., Tian, H., and Wang, J. (2015) A covalent approach for site-specific RNA labeling in mammalian cells. *Angew. Chem. Int. Ed. Engl.* **54**(15), 4597–4602.
21. Bracey, M. H., Christiansen, J., Tovar, P., Cramer, S. O., and Bartlett, S. G. (1994) Spinach carbonic anhydrase: investigation of the zinc-binding ligands by site-directed mutagenesis, elemental analysis, and EXAFS. *Biochemistry* **33**(44), 13126–13131.
22. Zhou, Z. S., Peariso, K., Penner-Hahn, J. E., and Matthews, R. G. (1999) Identification of the zinc ligands in cobalamin-independent methionine synthase (MetE) from Escherichia coli. *Biochemistry* **38**(48), 15915–15926.
23. Logan, D. T., Mulliez, E., Larsson, K. M., Bodevin, S., Atta, M., Garnaud, P. E., Sjöberg, B. M., and Fontecave, M. (2003) A metal-binding site in the catalytic subunit of anaerobic ribonucleotide reductase. *Proc. Natl. Acad. Sci. USA* **100**(7), 3826–3831.
24. Luttringer, F., Mulliez, E., Dublet, B., Lemaire, D., and Fontecave, M. (2009) The Zn center of the anaerobic ribonucleotide reductase from E. coli. *J. Biol. Inorg. Chem.* **14**(6), 923–933.
25. Bertini, I., Luchinat, C., and Monnanni, R. (1985) Zinc enzymes. *J. Chem. Educ.* **62**(11), 924–927.
26. Pace, N. J. and Weerapana, E. (2014) Zinc-binding cysteines: diverse functions and structural motifs. *Biomolecules* **4**(2), 419–434.
27. Zhang, Z., Yang, K., Chen, C. C., Feser, J., and Huang, M. (2007) Role of the C terminus of the ribonucleotide reductase large subunit in enzyme regeneration and its inhibition by Sml1. *Proc. Natl. Acad. Sci. USA* **104**(7), 2217–2222.
28. Berardi, M. J. and Bushweller, J. H. (1999) Binding specificity and mechanistic insight into glutaredoxin-catalyzed protein disulfide reduction. *J. Mol. Biol.* **292**, 151–161.
29. Edgar, R. C. (2010) Search and clustering orders of magnitude faster than BLAST. *Bioinforma.* **26**(19), 2460–2461.
30. Do, C., Mahabhashyam, M. S. P., and Batzoglou, S. (2005) ProbCons: Probabilistic consistency-based multiple sequence alignment. *Genome Res.* **15**(2), 330–340.
31. Criscuolo, A. and Gribaldo, S. (2010) BMGE (Block Mapping and Gathering with Entropy): a new software for selection of phylogenetic informative regions from multiple sequence alignments. *BMC Evol. Biol.* **10**, 210.
32. Stamatakis, A. (2014) RAxML version 8: a tool for phylogenetic analysis and post-analysis of large phylogenies. *Bioinforma.* **30**(9), 1312–1213.
33. Wheeler, T. J., Clements, J., and Finn, R. D. (2014) Skylign: a tool for creating informative, interactive logos representing sequence alignments and profile hidden Markov models. *BMC Bioinfo.* **15**(7).
34. Chou, P. Y. and Fasman, G. D. (1974) Conformational parameters for amino acids in helical, β-sheet, and random coil regions calculated from proteins. *Biochemistry* **13**(2), 211–222.
35. Chou, P. Y. and Fasman, G. D. (1974) Prediction of protein conformation. *Biochemistry* **13**(2), 222–245.
36. Arnold, K., Bordoli, L., Kopp, J., and Schwede, T. (2006) The SWISS-MODEL workspace: a web-based environment for protein structure homology modelling.. *Bioinforma.* **22**(2), 195–201.
37. Kiefer, F., Arnold, K., Kunzli, M., Bordoli, L., and Schwede, T. (2009) The SWISS-MODEL repository and associated resources. *Nucleic Acids Res.* **37**(Database issue), 387–92.
38. Guex, N., Peitsch, M. C., and Schwede, T. (2009) Automated comparative protein structure mod-

eling with SWISS-MODEL and Swiss-PdbViewer: a historical perspective. *Electrophoresis* **30 Suppl 1**, S162–173.

39. Biasini, M., Bienert, S., Waterhouse, A., Arnold, K., Studer, G., Schmidt, T., Kiefer, F., Gallo Cassarino, T., Bertoni, M., Bordoli, L., and Schwede, T. (2014) SWISS-MODEL: modelling protein tertiary and quaternary structure using evolutionary information. *Nucleic Acids Res.* **42**(Web Server issue), W252–8.
40. Holmgren, A. (1979) Thioredoxin catalyzes the reduction of insulin disulfides by dithiothreitol and dihydrolipoamide. *J. Biol. Chem.* **254**(19), 9627–9632.
41. Vlamis-Gardikas, A., Åslund, F., Spyrou, G., Bergman, T., and Holmgren, A. (1997) Cloning, overexpression, and characterization of glutaredoxin 2, an atypical glutaredoxin from Escherichia coli. *J. Biol. Chem.* **272**(17), 11236–11243.

FIGURES

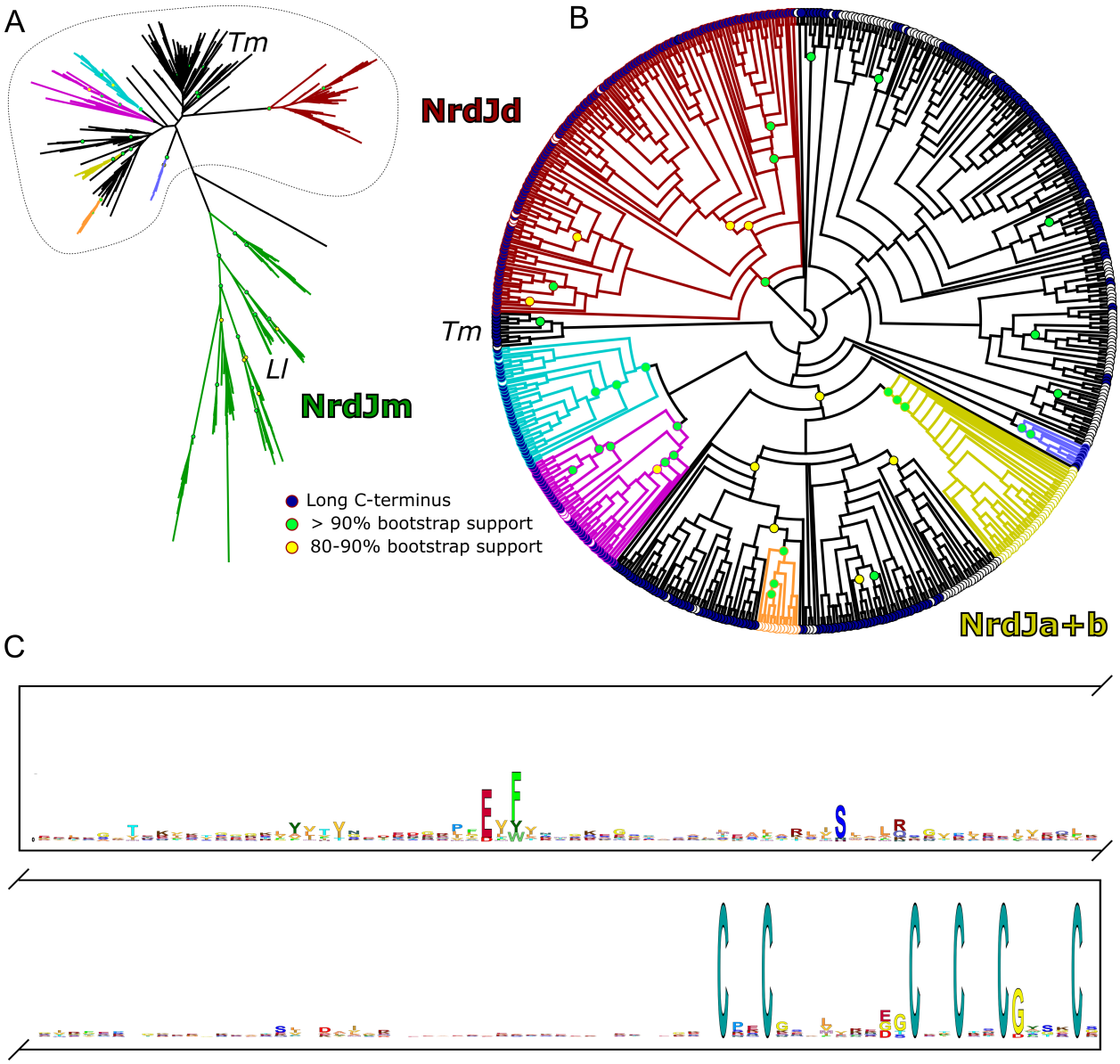

Figure 1: Phylogenetic analysis of NrdJ and sequence analysis of NrdJd. A) Maximum likelihood phylogenetic tree of a representative selection of NrdJ sequences. Subclasses with characterized members (NrdJm (green), NrdJd (red) and NrdJa+b (yellow)) and candidate subclasses (cyan, purple, orange and light blue) are indicated with color. *Lactobacillus leichmannii* RNR (Ll) is located in subclass NrdJm, while the RNR from *Thermotoga maritima* (Tm) is not part of a defined subclass B) Appearance of the Cysteine Rich Domain (CRD) mapped on a phylogenetic tree of a selection of non-monomeric NrdJ sequences. The selected subset is marked by the dotted line in panel A. Subclasses with characterized members (NrdJd (red) and NrdJa+b (yellow)) and candidate subclasses (cyan, purple, orange and light blue) are indicated with color. The presence of a CRD is indicated with a blue circle, absence with a white circle. The NrdJa+b suclass has the encoded CRD as a separate gene. C) Logo of the CRD derived from 217 non-redundant sequences from subclasses NrdJd and unclassified NrdJ.

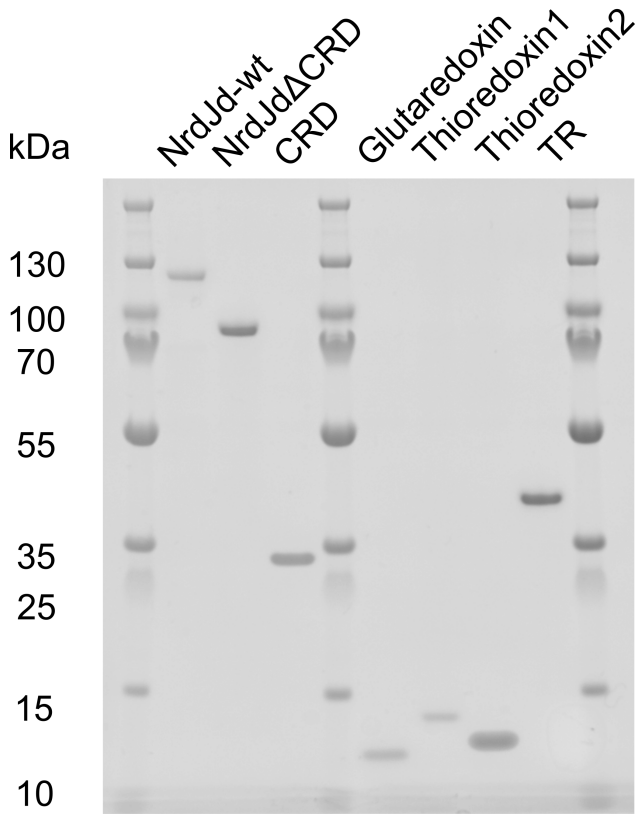

Figure 2: SDS-PAGE of the final purification of heterologously expressed *S. nassauensis* enzymes. Electrophoresis was performed with a 4-12% Bis-Tris Protein Gel. NrdJd-wt (Snas 4560): full length NrdJd enzyme (1-947); NrdJdΔCRD: C-terminal truncation without CRD (1-714), CRD: CRD of NrdJd (715-947), glutaredoxin (Snas 1785), thioredoxin 1 (Snas 2647), thioredoxin 2 (Snas 6430), TR: thioredoxin reductase (Snas 6431)

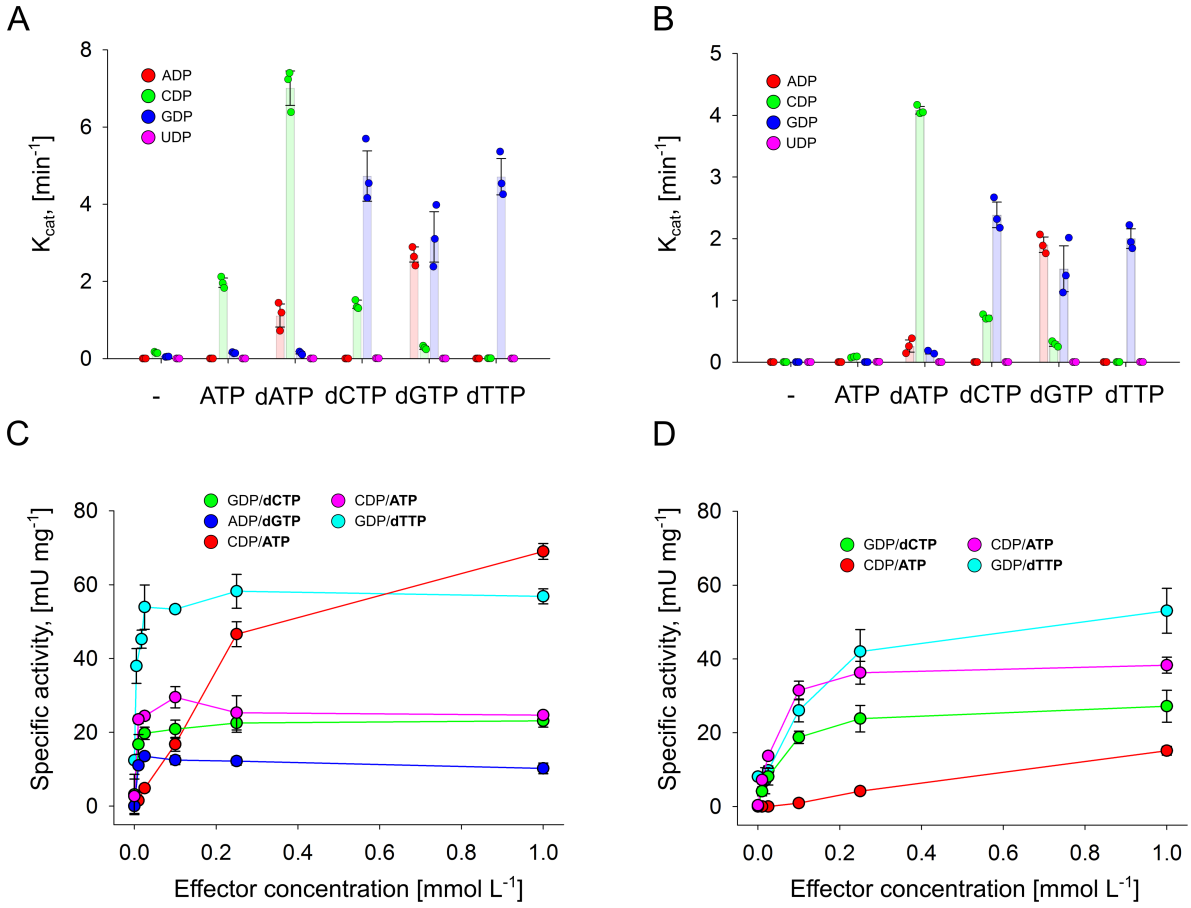

Figure 3: Activity of NrdJd-wt and NrdJdΔCRD in the presence of effector. A/B) Four substrate assay for NrdJd-wt (A) and NrdJdΔCRD (B) with or without effector. Each reaction contains the four potential substrates ADP, CDP, GDP and UDP plus one of the potential effectors dATP dCTP, dGTP, dTTP or ATP. C/D) Influence of the effector concentration on enzyme activity of NrdJd-wt (C) and NrdJdΔCRD (D) with one of the potential effectors dATP, dCTP, dGTP, dTTP or ATP. Titrations were performed in a concentration range from 4 to 1000 µmol L^{-1}, including a measurements without effector. Data where obtained in three independent experiments. Error bars indicate the standard deviation from the mean value.

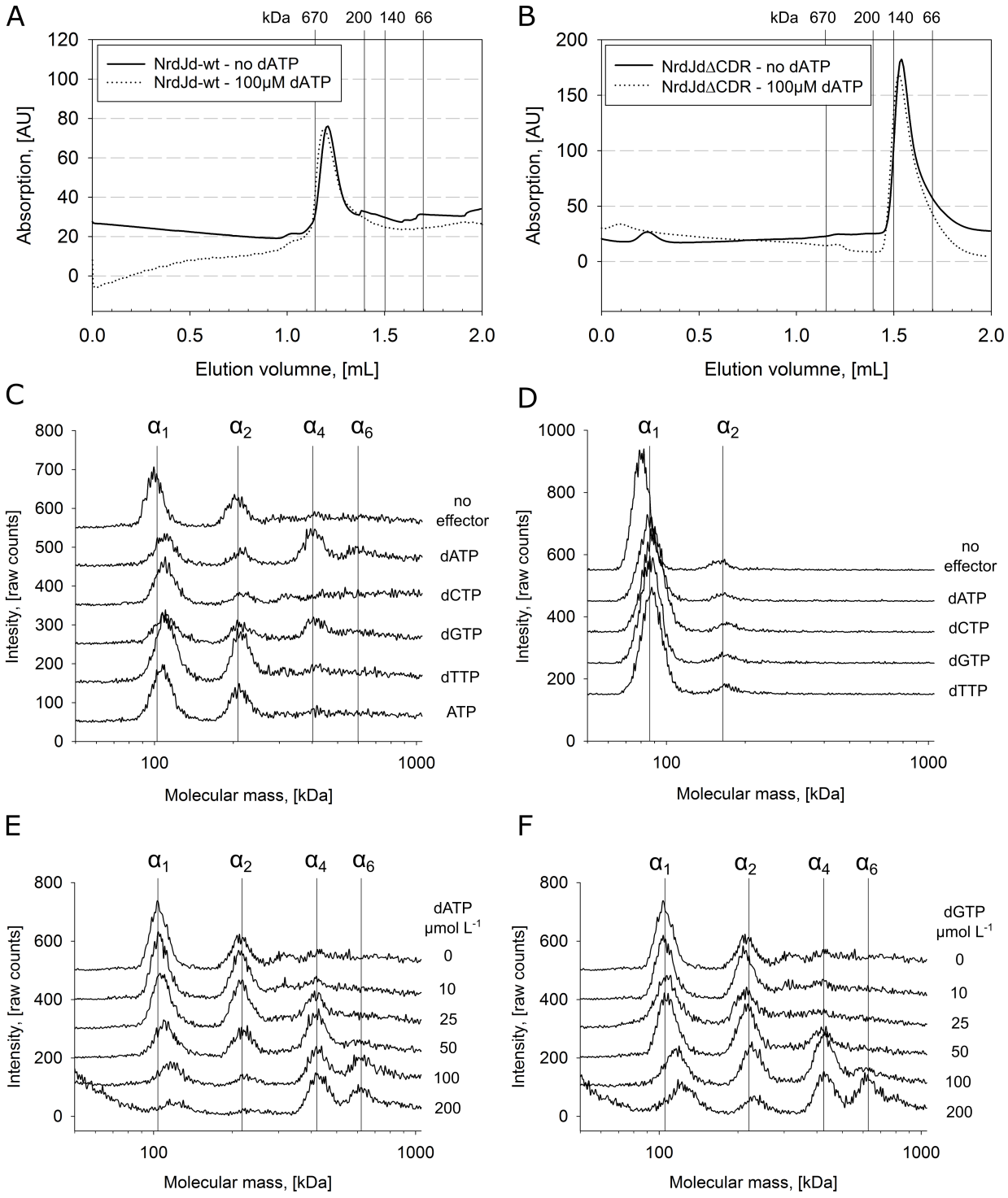

Figure 4: Oligomeric states of NrdJd and NrdJdΔCRD determined by SEC and GEMMA. Size exclusion chromatography of A) NrdJd-wt and B) NrdJdΔCRD with 1 mg mL^{-1} protein each. C) GEMMA experiments with 0.075 mg mL^{-1} NrdJd-wt and 100 µmol L^{-1} of one of the potential effectors. D) GEMMA experiment with 0.025 mg mL^{-1} NrdJdΔCRD and and 100 µmol L^{-1} of one of the potential effectors. E) GEMMA experiment with 0.075 mg mL^{-1} NrdJd-wt and a titration of the dATP concentration. F) GEMMA experiment with 0.075 mg mL^{-1} NrdJd-wt and a titration of the dGTP concentration. All GEMMA experiments represent 5 separate measurements for each condition.

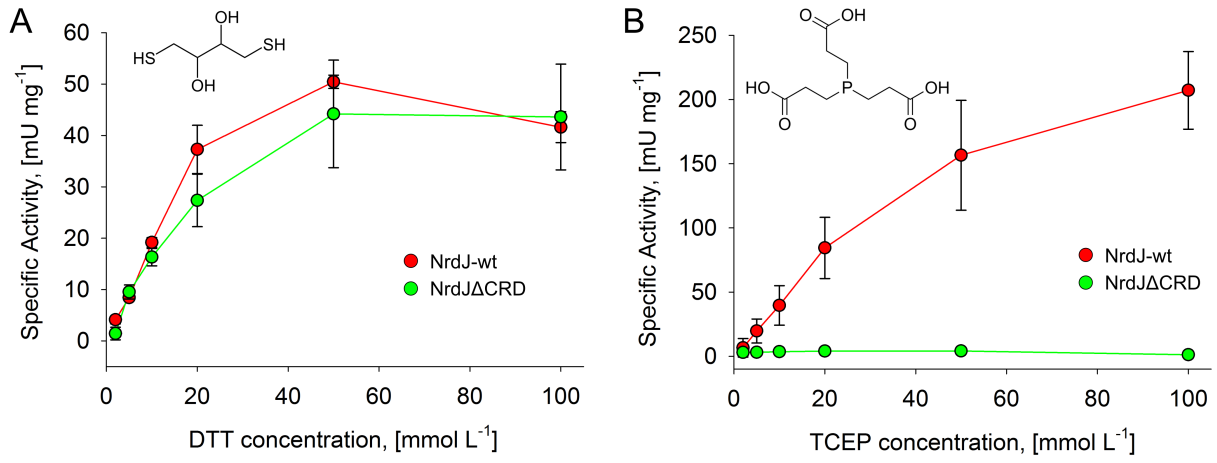

Figure 5: Reductant dependence of NrdJd and NrdJdΔCRD. Enzyme activity of NrdJd-wt (red) and NrdJdΔCRD (green) in the presence of different concentrations of the reductants A) DTT and B) TCEP. Assays were performed with CDP as substrate and dATP as effector. All experiments were performed in triplicates. Error bars indicate the standard deviation from the mean value.

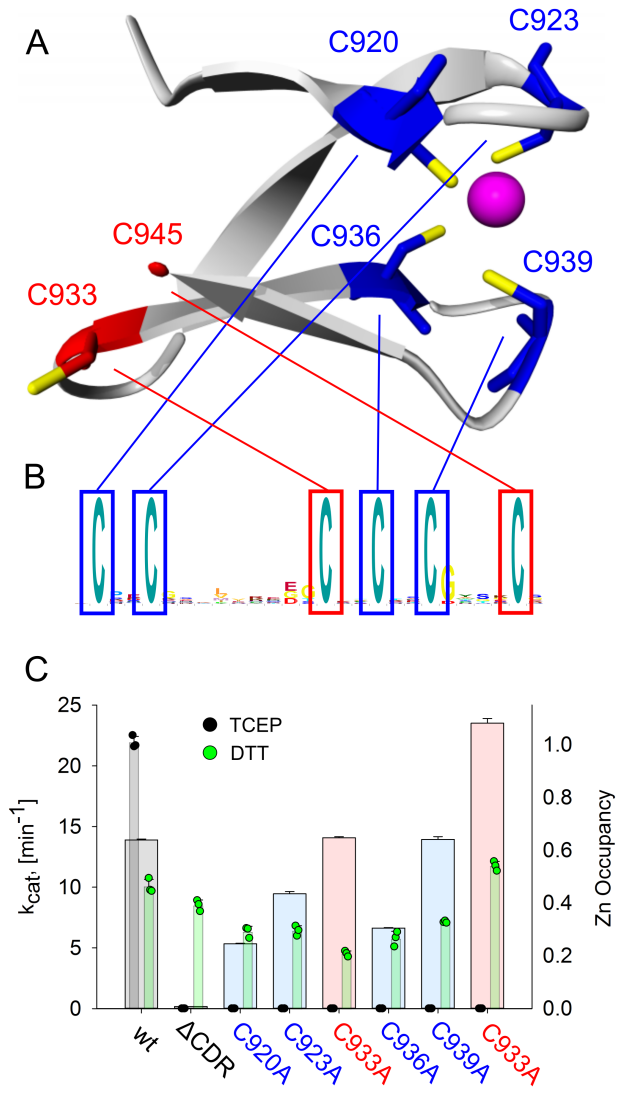

Figure 6: Homology model and biochemical characterization of the C-terminal zinc binding site. A) Homology model of the last 30 amino acids of the CRD from *S. nassauensis* NrdJd, based on the crystal structure of tRNA(Ile2) 2-agmatinylcytidine synthetase (PDB: 4RVZ) (20). B) Logo of the C-terminal end of *S. nassauensis* NrdJd-wt. C) Activities with the reductant TCEP (narrow bars; black) and DTT (narrow bars; green) and zinc content (broad bars) of NrdJd-wt and the cysteine to alanine variants. The colors red and blue refer to the predicted location of the respective cysteine residue. Data where obtained in three independent experiments. Error bars indicate the standard deviation from the mean value.

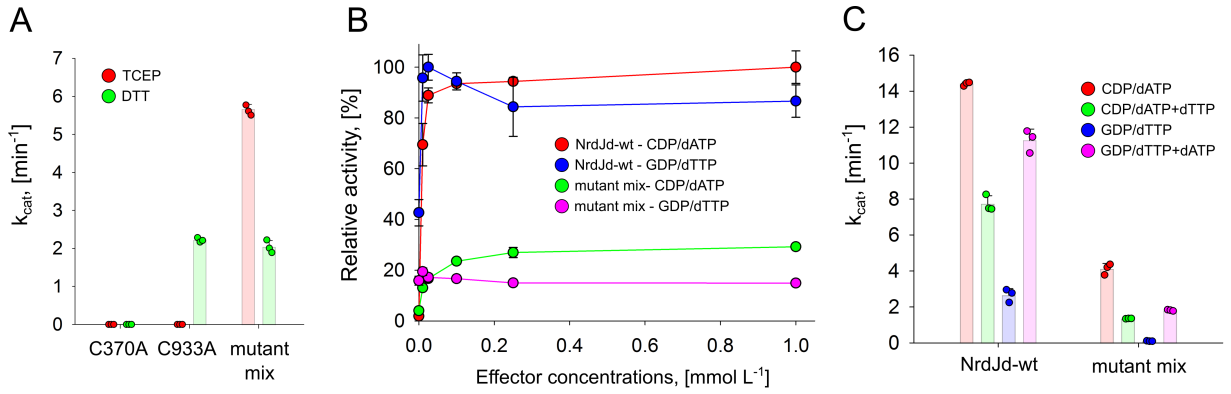

Figure 7: Enzyme activity of mixtures of mutant proteins. A) Specific activity per monomer of the C933A and C370A proteins tested individually and in an equimolar C933A/C370A mixture (mutant mix). B) Relative activities of NrdJd-wt and the mutant mix in effector titrations with the substrate effector pairs CDP/dATP (100% equals k_{cat} = 15.3 min^{-1}) and GDP/dTTP (100% equals k_{cat} = 3.1 min^{-1}) and TCEP as reductant. C) Activities of NrdJd-wt and the mutant mix with the substrates CDP or GDP and effector mixtures. TCEP was applied as reductant. Concentrations: dATP 250 μmol L^{-1}, dTTP 1 mmol L^{-1}. Data where obtained in three independent experiments. Error bars indicate the standard deviation from the mean value.

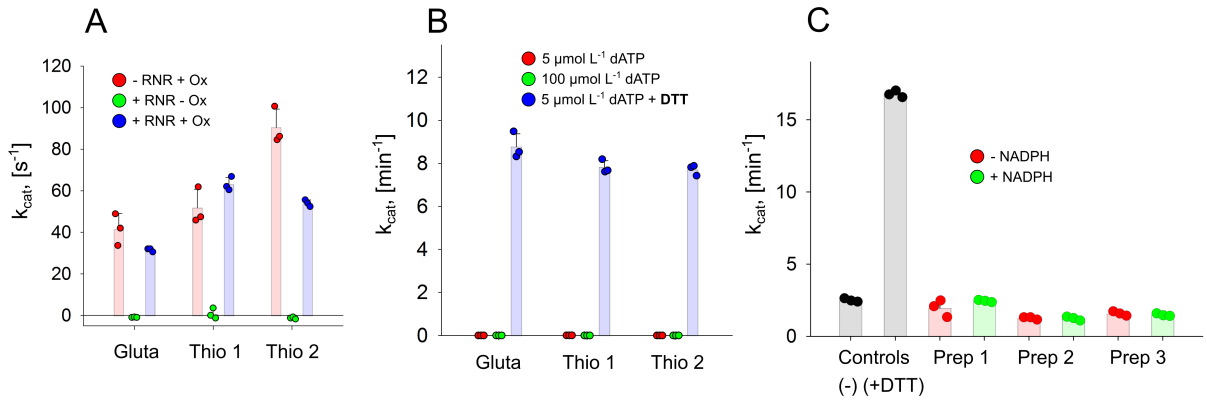

Figure 8: Activity assays in presence of potential native electron donor systems. A) Specific activity of glutaredoxin and the thioredoxins in the presence or absence of NrdJd-wt (+RNR and -RNR), respectively. The assays were performed with or without additional oxidant used as substrate (+Ox or -Ox). The additional oxidants were insulin for the thioredoxins and HED for glutaredoxin. B) Specific activity of NrdJd-wt in combination with glutaredoxin and the thioredoxins with the substrate CDP. C) Activity assays with NrdJd-wt in the presence of cell lysate preparations from *S. nassauensis* with (green) or without (red) 250 μmol L^{-1} NADPH addition: protein-free lysate (Prep 1), cleared lysate (Prep 2) and complete lysate (Prep 3). No artificial reductant such as DTT was added. As positive and negative controls, RNR-assays with (+DTT) and without (-) the reductant DTT were performed. RNR activity in the preparations and controls was determined by HPLC measurement of CDP consumption and dCDP synthesis. All data where obtained in three independent experiments. Error bars indicate the standard deviation from the mean value.

A unique cysteine-rich Zn-finger domain present in a majority of class II ribonucleotide reductases mediates catalytic turnover

Christoph Loderer, Venkateswara Rao Jonna, Mikael Crona, Inna Rozman Grinberg, Margareta Sahlin, Anders Hofer, Daniel Lundin and Britt-Marie Sjöberg

J. Biol. Chem. published online October 2, 2017
